JARO

Journal of the Association for Research in Otolaryngology

Organ of Corti Kinematics

Peter Dallos

Auditory Physiology Laboratory, The Hugh Knowles Center and Neuroscience Institute, Departments of Neurobiology and Physiology and Communication Sciences and Disorders, Northwestern University, Evanston, IL 60208, USA

ABSTRACT

The internal workings of the organ of Corti and their relation to basilar membrane motion are examined with the aid of a simple kinematic model. It is shown that, due to the lever system embodied in the organ of Corti, there is a significant transformer gain between basilar membrane and cilia displacements. While this transformation is nonlinear, linear response prevails in the narrow physiologically relevant operating range of the ciliary transducer. The model also simulates cilia deflection when the mechanical stimulus is the length change of outer hair cells.

Keywords: Organ of Corti, micromechanics, mechanical transformation, outer hair cell motility, cochlea models

INTRODUCTION

The past dozen years have brought remarkable advances in our understanding of the ear's operation. Of particular note are coherent, experimentally based theories of transduction and adaptation in hair cells, particularly as they pertain to nonmammalian vertebrates (for summaries see Hudspeth 1997a; Fettiplace and Fuchs 1999; Gillespie and Walker 2001). In addition, accurate and seemingly complete descriptions of basilar membrane motion patterns are now available for both the cochlear base and apex (for summary see Robles and Ruggero 2001). We also start to understand the molecular mechanisms of cochlear ho-

meostasis, fluid, and ion balance (for summary see Wangemann and Schacht 1996). Great strides have been made in identifying deafness genes, along with their phenotypes and appropriate mouse models (for summary see Steel and Kros 2001). The motor protein of outer hair cells, prestin, has been identified and some of its unique properties elucidated (for summary see Dallos and Fakler 2002). In spite of these advances, age-old questions remain unanswered. Those pertaining to the internal motions of elements of the organ of Corti are the subjects of this article.

COCHLEAR MICROMECHANICS

By definition, micromechanics describes the motions of elements of the organ of Corti and tectorial membrane that are a consequence of the presumed primary event: motion of the basilar membrane. The aim of micromechanics is to relate the final nonmolecular mechanical step, inner hair cell (IHC) ciliary displacement, to its precursor events. This inquiry dates back to ter Kuile (1900), with significant contributions by Békésy (1960). In spite of its hundred-year history, the subject is poorly understood, with experimental data being scarce, limited, and largely confined to preparations in nonphysiological condition. To dramatize the status of research on micromechanics, it is sufficient to note that there are no *in vivo* data available on the internal movements of the organ of Corti and that the prospect of seeing some soon is dim. This lack of information forces us to attempt to deduce intervening processes, aside from *in vitro* measurements, by comparing basilar membrane and neural (e.g., Narayan et al. 1998) or hair cell responses (e.g., Cheatham 1993).

Békésy emphasized the role of organ of Corti micromechanics in impedance matching. Contem-

Correspondence to: Peter Dallos · 2240 Campus Drive · Evanston, IL 60208. Telephone: (847) 491-3175; fax: (847) 467-4327; email: p-dallos@northwestern.edu
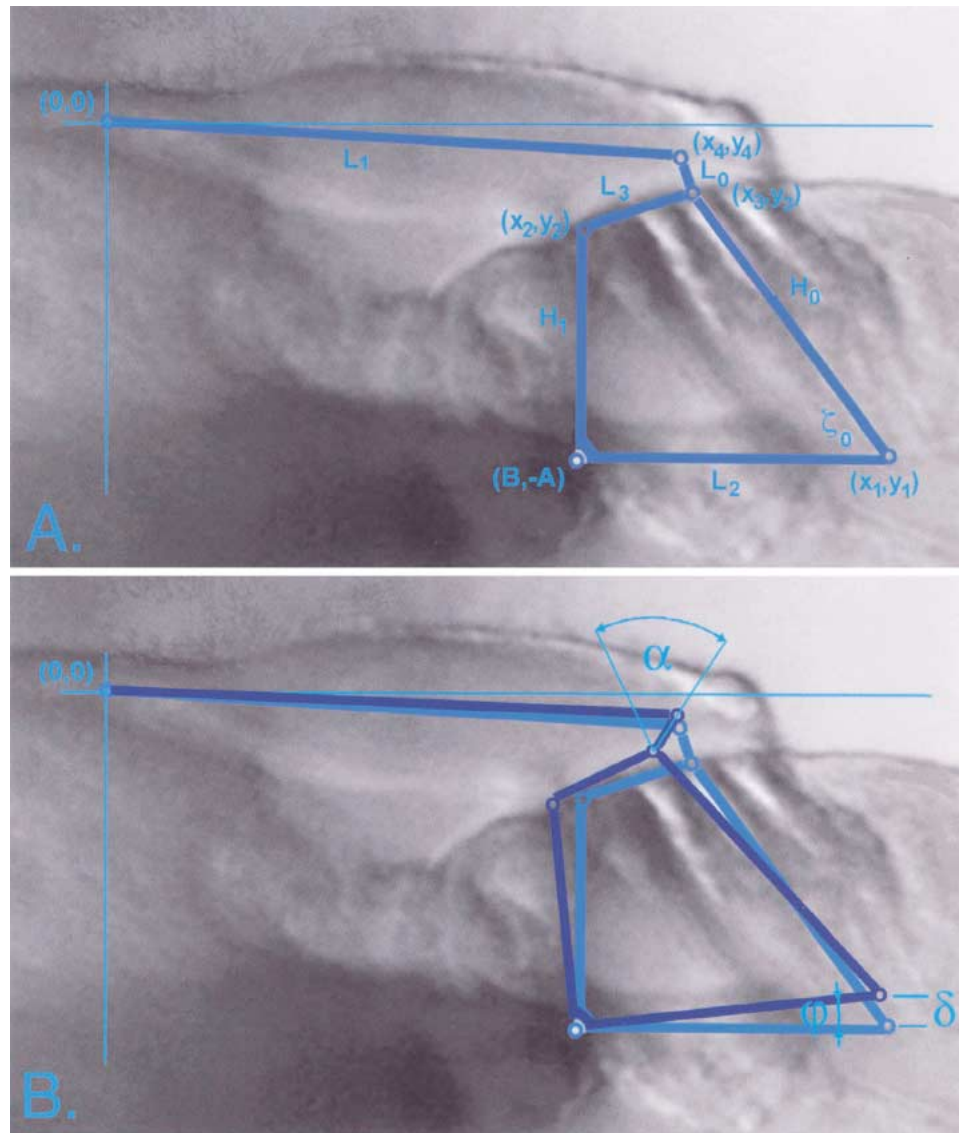
FIG. 1. Hemicochlea image of organ of Corti and tectorial membrane (TM) with critical elements represented as rigid, hinged beams. **A** Coordinate system is placed with its origin at the hinge point of the TM at the spiral limbus. Organ of Corti frame rotates around a hinge point (B,-A) where the basilar membrane (BM) meets the osseous spiral lamina. Combined pillar cells are represented by the beam H_1, perpendicular to the BM and rigidly tied to it. Three rows of OHCs and Deiters' cells are collapsed into a single beam (H_0), hinged to the BM at the location of the second row of OHCs and also to the reticular lamina (L_3). **B** indicates how the frame rotates when the BM displacement at the point of the attachment of H_0 is Δ. The BM, rotating as a rigid beam around its insertion point, subtends an angle Z when the BM is displaced by Δ. The result of this displacement is a change in cilia angle from its resting 90° to α.

porary formulations of his concern might pose two questions. Assuming that outer hair cell (OHC) somatic motility constitutes the cochlear amplifier (e.g., Dallos 1992; Nobili et al. 1998), how well-matched is the cells' mechanical impedance to that of the basilar membrane's? Similarly, if the reciprocal operation of hair cell transducer channels forms the basis of amplification (Hudspeth 1997b), what are the mechanical impedance relations among cilia and organ of Corti and basilar membrane? As a general question, reaching to the heart of inquiries about micromechanics, we need to know: are there multiple resonances, or multiple degrees of freedom, associated with the elements of the organ of Corti and tectorial membrane? This inquiry is usually answered in the affirmative (e.g., Allen 1980; Zwislocki 1980; Neely 1993; Gummer et al. 1996).

Whatever the dynamic properties of organ of Corti micromechanics may be, they modify a basic mechanical transformation between basilar membrane displacement and all other elemental displacements. Thus, the starting point for inquiries about organ of Corti micromechanics is an examination of displacement patterns when mass, stiffness, and damping are ignored and a rigid framework is substituted in lieu of critical structural components of the organ. This primitive approach has a hundred-year history (ter Kuile 1900). The most relevant antecedent is the computational model of Rhode and Geisler (1966) which is updated below. Those authors computed the relative displacement between two points situated opposite to one another on the reticular lamina (RL) and tectorial membrane (TM), respectively, as a function of basilar membrane (BM) displacement. Such a computation does not constrain cilia length and, consequently, it yields unrealistic results.

A simplified preliminary version of this material has been presented at the meeting: The Biophysics of

the Cochlea: From Molecule to Model, Titisee, Germany, 2002.

RESULTS AND DISCUSSION

Input: basilar membrane

We consider the relationship between basilar membrane displacement and cilia displacement. A simple representation of the mechanical system to be modeled is given in Figure 1A. A hinged but otherwise rigid framework is superimposed on a cross-section of the organ of Corti as seen in hemicochlea experiments (Edge et al. 1998). The basilar membrane (BM: L_2) and pillar cells (H_1) are represented as a rigid frame, hinged at the insertion into the osseous spiral lamina. The reticular lamina (RL: L_3) is assumed to be a rigid beam hinged at the top of the pillar cells. The tectorial membrane (TM: L_1) is also taken as a rigid beam; it rotates around its attachment at the spiral limbus. Multiple rows of outer hair cells (OHC) and Deiters' cells are collapsed and represented as a single beam, hinged at both of its extremes (H_0). This beam is placed at the location of the second row of OHCs. The resting angle between OHC/Deiters' cells and BM is Z_0. Finally, a single ciliary bundle (L_0) is hinged between RL and TM. All elements are assumed to be inertialess and no damping or elasticity is considered. A Cartesian coordinate system is placed so that the origin corresponds to the center of rotation of the TM at the spiral limbus. The two fixed centers of rotation are at coordinates $(0,0)$ and $(B,-A)$. All other hinge points move, as shown in Figure 1B. Dimensions used in subsequent computations are listed in Table 1. These dimensions for the three cochlear turns (approximate locations: 3, 6, and 10 mm from the base) of the gerbil are measured from magnified images obtained from unfixed hemicochlea material (Edge et al. 1998; Richter et al. 2000; and unpublished data). Cilia height is taken from Wright (1984) and Strelioff and Flock (1984). Cilia dimensions are not available for the gerbil. As shown in Figure 1B, the input is a linear deflection of the basilar membrane under the OHC (Δ), while the output is the angular position of the cilia (α; note that we make the assumption that in their resting position the cilia are perpendicular to the RL).

As the BM is deflected by Δ (or, equivalently, as the BM angle becomes φ) the bottom of the cilium moves from its resting coordinate (X_{30}, Y_{30}) to a new location (X_3, Y_3). To obtain the coordinates of this new position, one solves the simultaneous equations for the intersection of two circles, one formed by the rotation of the RL around the coordinate point (X_2, Y_2), the other by the rotation of the OHC/Deiters' cell beam

TABLE 1

Organ of Corti dimensions for adult gerbils derived from unfixed hemicochlea images (Edge et al. 1998, Richter et al. 2000 and unpublished material)

	Basal turn	Middle turn	Apical turn
A (μm)	68	97	93
B (μm)	95	122	118
L_0 (μm)[a]	1.6	2.9	5
L_1 (μm)	97	165	160
L_2 (μm)	53	103	117
L_3 (μm)	18	40	50
H_0 (μm)	72	110	113
H_1 (μm)	57	80	77
ζ_0 (degree)	58	57	53

[a]Cilia dimensions (L_0) are from Strelioff and Flock (1984) and Wright (1984). See Figure 1A for nomenclature.

around (X_1, Y_1). Once (X_3, Y_3) is obtained, the coordinates of the top of the cilia (X_4, Y_4), may be computed in a similar manner. These coordinates are also obtained from the intersection of two circles: one centered at (X_3, Y_3) and having a radius of L_0 and the other, centered at the origin with a radius of L_1. Because the analytical solution is complex and unwieldy, we demonstrate numerical results obtained with Mathematica® (Wolfram Research, Inc., Champaign, IL). In as much as there are several solutions, the proper ones need to be selected on the basis of physical realizability and correct provision of resting coordinates.

Figure 2 demonstrates some computational results for three cochlear locations. In the top panel, the change in cilia angle (from the resting 90°) is given as a function of BM displacement (Δ). The middle panel gives angular gain (in dB), obtained as the ratio of cilia angle (α) and BM angle (Z) at a given Δ. Finally, in the bottom panel the ratio of cilia angle change and BM displacement is plotted. Visual inspection of any of the plots suggests that the transformation between BM and cilia motions is nonlinear. Specifically, the gain of angular rotations is not constant, it becomes larger with increasing BM displacement. The basic character of computed responses is the same for all three cochlear locations. There are, however, obvious quantitative differences, reflecting the changing geometry along the length of the cochlea. More basal locations present higher gain and more restricted operating ranges. Further, angle change and gain are not symmetrical for positive and negative displacements of the BM.

We also note that the range of BM deflections is severely limited. This is imposed by the geometry of the structure and, more importantly, by the known range of angular rotations of the ciliary bundle between the limits where most mechano-transducer
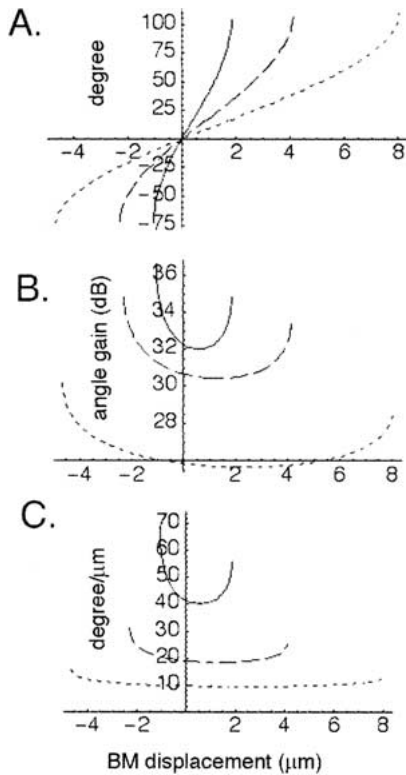
FIG. 2. Computational results for three cochlear locations using the parameters listed in Table 1. **A**. Cilia angle change (α in degrees) in response to BM displacement (Δ in micrometers). **B**. Ratio of cilia angle and basilar membrane angle (α/Z, expressed in decibels).**C**. Ratio of cilia angle and BM displacement (α/Δ, expressed in degrees/micrometer).

channels are either open or closed (Hudspeth and Corey 1977). Consider the second limitation first. To demonstrate this, an OHC transducer function is reproduced from the data of Kros et al. (1995) in Figure 3A. Essentially the full dynamic range of the cell is covered over ~2° angular displacement of the cilia. In Figure 3B a representation of the basal-turn computations is reproduced from Figure 2A and shown on an expanded scale in Figure 3C. The scale in Figure 3C is chosen to cover the ~2° operating range. The corresponding functional range of BM displacements is between approximately −10 and +40 nm, a remarkably small excursion. For the basal-turn location, the angular gain, α/Z, is ~32 dB at small displacements, and the ratio of angle change and BM displacement is ~40°/μm. These numbers reflect the operation of the BM/organ of Corti system as a mechanical transformer with a large transformer ratio. The system is a compound lever with the output arm, the cilia, being very short in comparison to the input arm—the driving organ of Corti frame. As a consequence, the transformer gain is significant and small BM rotation causes large angular displacement of the cilia. Within the limited operating range of the

transducer channels in the stereocilia bundle, the relationship between cilia angle and BM displacement is linear (Fig. 3C). Aside from considering limitations on motion imposed by the nature of the transducer channel (Fig. 3), BM displacement is clearly restricted by the asymptotic limit of $\alpha \rightarrow \pm 90°$. This can be seen in Figure 2A, where for any turn the plots approach the vertical. The implication is that basilar membrane displacements in excess of a few micrometers would probably cause severe structural disruption of the transducer apparatus in the cilia and probably other damage as well. Judging from the literature, experimental stimulation or micromanipulation of the BM exceeding the apparent safe range is not uncommon.

Finally, it is also noted parenthetically that a simple approximation of cilia angle may be had by assuming that it is only the radial motion of the bundle's base that causes the angle change; in other words, if the rotation of the RL about the pillar heads is ignored. In this case, $\alpha \approx \cos^{-1}[H_1(\sin Z)/L_0] = \cos^{-1}[H_1\Delta/L_0 L_1]$. Plots based on this approximation are included in Figure 3B,C as thin lines.

Input: OHC motility

Next, we ask what happens if the driving force comes not from the BM but from "active" OHCs, as if these cells were electrically stimulated to produce motility. In the configuration of Figure 1, it is apparent that OHC elongation rotates the reticular lamina counterclockwise, while it pushes the basilar membrane toward scala tympani. The latter motion attempts to displace the reticular lamina toward the periphery of the organ of Corti. Thus, in the simple configuration modeled here, two opposing actions result from OHC contraction/elongation cycles. However, in the real cochlea OHC length change does not move RL and BM by the same amount. Because the stiffness of the BM is greater than that of the RL, the latter moves with greater amplitude. The one available comparison, made for the apex of the guinea pig, reveals a ratio of displacements of BM to RL of approximately 1/5 (Mammano and Ashmore 1993). Thus, the RL moves in excess of the BM. We define the number M as the ratio of BM displacement to total displacement. Thus, if BM and RL move the same amount under electrical stimulation of OHC motility, M = 1/2. For the Mammano and Ashmore (1993) data, M = 1/6. This ratio is incorporated in our calculations, for all three turns, in which superposition is used to obtain cilia-angle change. We perform the computations as if two modes of stimulation summed their effects. Assume that the total change in length of OHC/Deiters' cell (H_0) is d. In the first mode of excitation, the OHC/Deiters' cells length is altered by an amount $d(1-M)$, while the BM
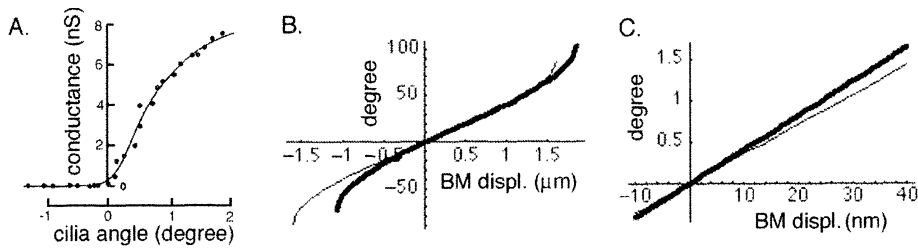
FIG. 3. **A**. Transducer conductance as a function of cilia displacement angle (modified from Kros et al. 1995). **B**. Basal turn response is replotted (heavy line) from Figure 2A, along with the results of an approximate computation (thin line); see text. **C**. A restricted portion of the curves from **B** is shown to correspond to the dynamic range of cilia deflections as gleaned from **A**.
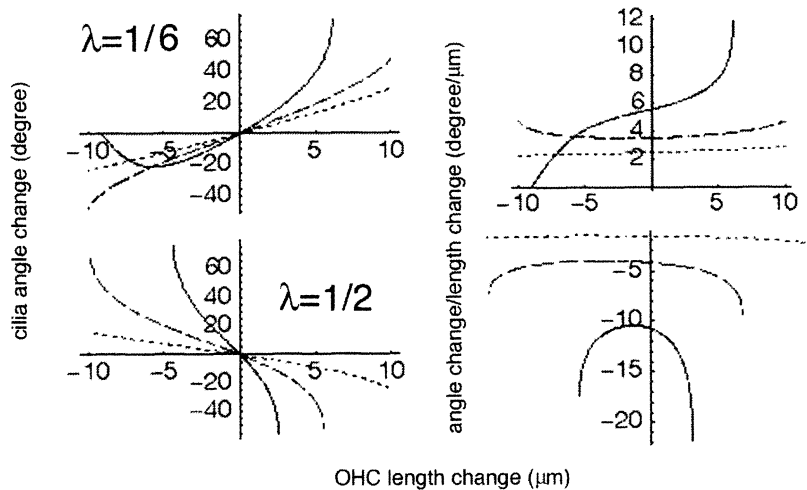

FIG. 4. Computational results for the case where excitation is due to OHC length changes. Left column: cilia-angle change (α in degrees), right column: cilia-angle change divided by OHC length change (α/d in degrees/micrometer). Two cases are shown. On the top, the RL moves five times the displacement of the BM. This corresponds to the measurements of Mammano and Ashmore (1993). On the bottom, computational results are shown for equal motion of BM and RL.

is kept stationary ($\Delta = 0$). In the second mode, the BM is displaced by an amount $\Delta = -Md \sin Z_0$: a motion component perpendicular to the BM. The top two panels in Figure 4 show cilia angle change (left) and ratio of cilia angle change to OHC elongation (right). The slopes are generally positive, signifying the dominance of RL rotation in producing a response. Response character is somewhat different between basal and apical turns. However, for realistic length changes, confined within ±3 µm, the responses are similar for all three locations, albeit the gain is different. For the basal turn, a 1-µm length change of the OHC produces ~6° cilia-angle change. It is recalled that the sensitivity of the motile response is ~20 nm/mV for an unloaded OHC. Consequently, a 1-mV OHC membrane potential change is expected to produce up to ~0.12° cilia rotation.

It should be emphasized that the computed responses are highly sensitive to the assumed ratio of BM and RL displacements. As an example, we show the M = 1/2 case, that is, for the hypothetical situation where the active OHC moves the RL and the BM equally but in opposing directions. In the lower panels of Figure 4, the results are shown. In this case, the dominant effect is due to the motion of the BM, hence the negative sign for the gain function. Comparison of the gain plots for M = 1/2 and 1/6 reveals the complexity of this mode of stimulation, radical dependence on the relative mobility of RL and BM, and the significant differences among turns.

Finally, in the kinematic organ of Corti representation, the gain of reverse transformation from single hair cell ciliary angle change (α) to reticular lamina radial displacement is ~$L_0 \sin \alpha$. Thus, at a basal-turn location, a 1° rotation of the bundle would produce an ~28-nm radial reticular lamina displacement at the base of the ciliary bundle. This produces a corresponding ~25-nm basilar membrane movement.

CONCLUSIONS

In this work I studied the relationship between stereocilia deflection and basilar membrane displacement. A greatly simplified kinematic model was examined. It is emphasized that the approach presented here is at best a first approximation. Obviously, the organ of Corti—basilar membrane–tectorial membrane system is not constituted of rigid beams. If bending of the ''beams'' is allowed, the computed gain is reduced. This reduction, however, is unlikely to be large. Furthermore, the kinematic approach permits the examination of motions at DC only. Finally, the computations represent the ''open loop'' case in the absence of any form of cochlear amplification, be it due to somatic or ciliary motility.

Several conclusions arise from the use of the model. First, due to the floating lever system embodied in the organ of Corti elements, there is a significant transformer action present, as envisioned by Békésy (1960). The transformer gain was estimated for the basal turn as ~40° cilia-angle change for each micrometer of basilar membrane displacement (Fig. 3B). The consequence of this high gain is a limited permissible dynamic range of basilar membrane deflections, if cilia motion is to be maintained within its normal operating range of ~ ±1–2°.

Further considerations indicated that somatic motility of OHCs could produce cilia deflection, with an estimated gain of up to 0.13°/mV membrane potential change. At acoustic threshold, the OHC receptor potential is ~1 mV and the basilar membrane displacement is ~2 nm. The latter corresponds to a computed cilia angle of 0.08°; this value should be compared with that produced via OHC somatic motility by a −1-mV receptor potential, i.e., ~0.13°. Clearly, OHC motile responses can be effective. As the simple calculations show, cilia rotation can also provide an effective input, displacing both the reticular lamina and the basilar membrane.

ACKNOWLEDGMENTS

REFERENCES

ALLEN JB. Cochlear micromechanics—a physical model of transduction. J. Acoust. Soc. Am. 68:1660–1670, 1980.

BÉKÉSY G. Experiments in Hearing.McGraw-Hill, New York, pp 745, 1960.

CHEATHAM MA. Cochlear function reflected in mammalian hair cell responses. Progr. Brain Res. 97:13–19, 1993.

DALLOS P. The active cochlea. J. Neurosci. 12:4575–4585, 1992.

DALLOS P, FAKLER B. Prestin, a new type of motor protein. Nat. Rev. Mol. Cell. Biol. 3:104–111, 2002.

EDGE RM, EVANS BN, PEARCE M, RICHTER C-P, HUX X, DALLOS P. Morphology of the unfixed cochlea. Hear. Res. 124:1–16, 1998.

FETTIPLACE R, FUCHS PA. Mechanisms of hair cell tuning. Ann. Rev. Physiol. 61:809–834, 1999.

GILLESPIE PG, WALKER RG. Molecular basis of mechanosensory transduction. Nature 413:194–202, 2001.

GUMMER AW, HEMMERT W, ZENNER H-P. Resonant tectorial membrane motion in the inner ear: its crucial role in frequency tuning. Proc. Natl. Acad. Sci. USA 93:8727–8732, 1996.

HUDSPETH AJ. How hearing happens. Neuron 19:947–950, 1997a.

HUDSPETH AJ. Mechanical amplification of stimuli by hair cells. Curr. Opin. Neurobiol. 7:480–486, 1997b.

HUDSPETH AJ, COREY DP. Sensitivity, polarity, and conductance change in the response of vertebrate hair cells to controlled mechanical stimuli. Proc. Natl. Acad. Sci. USA 74:2407–2411, 1977.

KROS CJ, LENNAN GWT, RICHARDSON GP. Transducer currents and bundle movements in outer hair cells of neonatal mice. In: FLOCK Å, OTTOSON D, ULFENDAHL M (eds) Active hearing. Elsevier Science, Oxford, pp 113–125, 1995.

MAMMANO F, ASHMORE JF. Reverse transduction measured in the isolated cochlea by laser Michelson interferometry. Nature 36:838–841, 1993.

NARAYAN SS, TEMCHIN AN, RECIO A, RUGGERO MA. Frequency tuning of basilar membrane and auditory nerve fibers in the same cochleae. Science 282:1882–1884, 1998.

NEELY ST. A model of cochlear mechanics with outer hair cell motility. J. Acoust. Soc. Am. 94:137–146, 1993.

NOBILI R, MAMMANO F, ASHMORE J. How well do we understand the cochlea? Trends Neurosci. 21:159–167, 1998.

RHODE WS, GEISLER CD. Model of the displacement between opposing points on the tectorial membrane and reticular lamina. J. Acoust. Soc. Am. 42:185–190, 1966.

RICHTER C-P, EDGE R, HE DZZ, DALLOS P. Development of the gerbil inner ear observed in the hemicochlea. J. Assoc Res. Otolaryngol. 1:195–210, 2000.

ROBLES L, RUGGERO MA. Mechanics of the mammalian cochlea. Physiol. Rev. 81:1305–1352, 2001.

STEEL KP, KROS CJ. A genetic approach to understanding auditory function. Nat. Gen. 27:143–149, 2001.

STRELIOFF D, FLOCK Å. Stiffness of sensory-cell hair bundles in the isolated guinea pig cochlea. Hear. Res. 15:19–28, 1984.

TER KUILE E. Die Übertragung der Energie von der Grundmembran auf die Haarzellen. Pflüg. Arch. Ges. Physiol. 79:146–157, 1900.

WANGEMANN P, SCHACHT J. Homeostatic mechanisms in the cochlea. In: DALLOS P, POPPER AN, FAY RR (eds) The Cochela Springer, New York, pp 130–185, 1984.

WRIGHT A. Dimensions of the cochlear stereocilia in man and the guinea pig. Hear. Res. 13:89–98, 1984.

ZWISLOCKI JJ. Five decades of research on cochlear mechanics. J. Acoust. Soc. Am. 67:1679–1685, 1980.